Talanta 233 (2021) 122515

Contents lists available at ScienceDirect

Talanta

journal homepage: www.elsevier.com/locate/talanta

A general scattering proximity immunoassay with the formation of dimer of gold nanoparticle

Hong Zhou [a,*], Qiao Yu [b], Haiyan Wang [d], Wenjing Zhu [e], Jing Liu [c,**], Zonghua Wang [b]

[a] Key Laboratory of Optic-electric Sensing and Analytical Chemistry for Life Science, Ministry of Education, College of Chemistry and Molecular Engineering, Qingdao University of Science and Technology, Qingdao, 266042, PR China
[b] Shandong Sino-Japanese Center for Collaborative Research of Carbon Nanomaterials, College of Chemistry and Chemical Engineering, Qingdao University, Qingdao, Shandong, 266071, PR China
[c] College of Chemical and Biological Engineering, Shandong University of Science and Technology, Qingdao, Shandong, 266590, PR China
[d] The Affiliated Hospital of Qingdao University, Qingdao, Shandong, 266071, PR China
[e] Department of Pharmacy, Qingdao Municipal Hospital, School of Medicine, Qingdao University, Qingdao, Shandong, 266071, PR China

ARTICLE INFO

Keywords:
Oriented assembly
Au NPs dimers
Dark-field imaging
Proximity binding-based immunoassay
Colorimetric biosensor

ABSTRACT

In this work, we structured a colorimetric ultrasensitive detection of carcinoembryonic antigen (CEA) based on a proximity hybridization-induced gold nanoparticles (Au NPs) dimers structure. Under the dark-field microscope, this method takes advantage of the distinctive and strong distance-relative localized surface plasmon resonance (LSPR) of Au NPs and their oriented assembly. DNA served as a medium showing wonderful flexibility to label antibody and Au NPs, and tune interparticle spacing as well. Two capture probes were formed by the integration of DNA labeled antibody (DNA1-Ab1 or DNA2-Ab2) and asymmetrically assembled DNA (DNA 3 or DNA 4)- Au NPs *via* partly hybridization between DNA sequences. In the presence of antigen, the reaction between target protein and capture probes could trigger the generation of immunocomplex which led to the proximity hybridization of the DNA1 and DNA2, and then change the distance of interparticle to form Au NP dimers and thus showed a different color under dark-field microscope. A limit of detection of 14.25 pg/mL was obtained for the detection of CEA, which indicated a promising sensing method in clinical diagnosis of protein biomarkers.

1. Introduction

Sensitive and specific detection of protein biomarkers shows significant application in the field of clinical disease monitoring, diagnosis and treatment. Immunoassay methods which rely on the specific binding between antibody and antigen is one of most widely used methods for protein biomarkers detection. Among immunoassay methods, proximity binding-based immunoassay, first developed by Landegren and co-workers in 2002 [1], has attracted rising attention for clinical biomarkers detection. In these proximity binding immunoassay methods, aptamers or antibody modified DNA pairs were generally employed. The formation of sandwich immunocomplexes results in close proximity between the tail sequences of aptamers or DNA pairs. This provides an increased concentration and allows subsequent DNA hybridizations [2,3]. One of advantages here is that the detection process is carried out in homogeneous solutions with no multiple separation or washing steps. During the process, the affinity recognition from target proteins can be converted to DNA signal outputs, which greatly enhanced the sensitivity in comparison to that of conventional enzyme-linked immunosorbent assay (ELISA). To now, proximity binding-immunoassay approaches have been widely developed and have been successfully applied for sensitive detection of various protein biomarkers *via* different means, such as electrochemical [4] or electrochemiluminescence method [5,6], fluorescent [7,8], colourimetric [9], chemiluminescent (CL) [10,11] and photoelectrochemical [12] etc. In order to further enhance the sensitivity, DNA-based isothermal amplification strategies [13–16] have been employed in the proximity binding-based immunoassay. However, the involvement of enzymes and incubation equipment in thermal cycle amplifications greatly increased the cost and complexity of these detection methods.

To solve above problems, a new sensing method named scattering-based dark field imaging method has been reported for individual

* Corresponding author.
** Corresponding author.
E-mail addresses: zhouhong@qust.edu.cn (H. Zhou), jliu99@126.com (J. Liu).

https://doi.org/10.1016/j.talanta.2021.122515
Received 3 November 2020; Received in revised form 2 April 2021; Accepted 9 May 2021
Available online 26 May 2021

nanoparticle imaging in the field of biosensing applications. This new method provides better performance comparing with traditional sensing methods due to its unique simplicity and ultrahigh sensitivity of the darkfield microscope technique [17–25]. Unlike traditional bulk measurement, imaging process from darkfield microscope technique focuses on the signal generated by individual particles platforming the system. By virtue of dark-field imaging, there are three kinds of methods have been developed for quantitative purposes. Firstly, the spectral shift-based approaches, through tracking single particles and collecting the plasmon resonance spectrum, quantify the target on the basis of spectral shift of particles. However, it cannot be ignored that particle properties, such as size and morphology, are directly associated with the spectrum. Secondly, the scattered intensity-based means depends on the change of intensity of scattered light before and after the addition of analyte. Finally, a newly emerged strategy called particle enumeration correlates the amount of particle with the number of target molecules, which is invisible resorting to the dark-field microscope. Since particle-counting approach can lower the interference from glass slide or sample matrix, on some degree, it is potential to be applied in practice. However, the Au NP counting technique is generally limited to single Au NP or Au NP dimers-based quantification from the analytes. It is not effective for the counting of Au NP trimers or tetramers, etc.

To circumvent this problem, in this work, we employed single asymmetrically modified Au NPs as independent monomer probes for accurate and sensitive quantifying CEA in homogeneous solutions. Au NPs, coating with dense thiolated PEG and sparse DNA3 hybridized with DNA1 modified the detection antibody (Ab1) to the formation of captured probe (probe1) for the part complementation of DNA1 and DNA3. Meanwhile, asymmetrical modification AuNPs with thiolated PEG and DNA4 react with DNA2 modified the detection antibody (Ab2) to obtain probe 2. The reaction of antigens (CEA) with antibody (probe 1 and probe 2) gives rise to the generation of Au NPs dimers along with a green-to-yellow color change under dark-field microscope, resulting in the increase of yellow spots. Due to asymmetric modification and steric hindrance effect, in the presence of the target CEA, Au NPs can only form dimers, but not trimers, tetramers, etc. The formation of dimer induced a plasmon resonance coupling effect, and this further results in a significant scattering signal and the sensitivity of detection is greatly improved.

2. Experimental section

2.1. Materials

50 nm spherical AuNPs was provided by BBI solutions (Cardiff, U.K.). Tris (2-carboxyethyl) phosphine hydrochloride (TCEP), dithiothreitol (DTT), sulfosuccinimidyl-4-(N-maleimidomethyl)-cyclohexane-1-carbo xylate (SMCC) and O-(3-Carboxypropyl)-O′-[2-(3-mercaptopropionylamino) ethyl]-polyethylene glycol (MW 3000, SH-PEG-COOH) were purchased from Sigma-Aldrich. Anti-CEA (Catalog L1C00205), Anti-CEA (Catalog L1C00202) and CEA (Catalog LC01001) were obtained from Shanghai Linc-Bio Science Co. Ltd. (Shanghai, China). DNA sequences (DNA1, DNA2, DNA3, DNA4 and DNA5) were supplied by Takara Biotechnology (Dalian China). The sequence of oligonucleotides in detailed are as follows:

DNA1: 5′-ACTCCGATCAGGTATGCCAGCAAGACTTTTTTTATCACAT CAGG.

CTCTAGCGTATGCTATTG-SH -3’.

DNA2: 5′-SH-GTTATCGTATGCGATCTCGGACTACACTATTTTTTTG TCTTG.

GACAGTGCTAGTGCTGCACG -3’.

DNA3: 5′- SH-TTTTTTCTGGCATACCTGATCGGAGT -3’.

DNA4: 5′- CGTGCAGCACTAGCACTGTCTTTTTT-SH -3’.

DNA 5: 5′-SH-TTTTTTCTGGCAATACCTGATCGGAGT-FAM- 3’.

2.1.1. Instrumentation

UV–vis absorption spectra and the fluorescence emission spectra of Au NPs were respectively studied using UV–vis spectrophotometer (Nanodrop-2000C, USA) and F-4600 Fluorescence Spectrophotometer (HITACHI, Japan). The ζ potential and size of Au NPs before and after modification were recorded using Nano ZS90 (Malvern, Britain). Darkfield microscopic images were inquired with optical microscope (IX73, Olympus, Japan) and processed by Image-Pro Plus 6.0. The measurement of morphology of nanomaterials was conducted by JEM-2100 Transmission electron microscope (HITACHI, Japan).

2.2. Preparation of asymmetrical modification Au NPs with PEG

The asymmetrically modified Au NPs with PEG were prepared according to the methods reported previously with a slight modification [23,26]. 1.0 mL Au NPs (50 nm) was doped on glass glide for 4 h based on electrostatic attraction, followed with thoroughly washing with distilled water and immersed in 10 μM thiolated PEG overnight. After ultrasonic treatment, asymmetry-PEGylated Au NPs were removed from glass glide, centrifuged (8000 rpm, 10min) and washed with distilled water three time. Finally, the pellet at the bottom was resuspended in Tris-HCL (pH 7.4) buffer. According to the UV–vis absorbance intensity in Fig. S1, the concentration of Au-PEG was 27.37 pM after asymmetrical modification with PEG.

2.3. Preparation of DNA-labeled asymmetry-PEGylated Au NPs

DNA3 and DNA4 was deprotected by virtue of TCEP to reduce the disulfide bonds. 9.49 μL DNA 3 and DNA 4 was separately added into 100 μL asymmetrical Au NPs at room temperature for 12 h, then the obtained solution was centrifuged and the supernatant was removed to get rid of excessive mountain of DNA. Subsequently, the particles were resuspended in buffer solution.

2.4. Preparation of DNA-labeled antibody

4 μL 100 mM DTT solution was added into 4 μL 100 μM DNA1 PBS solution (55 mM phosphate containing 50 mM NaCl and 20 mM EDTA , pH = 7.4) and kept at 37 °C for 1.0 h. 2.46 μL antibody1 solution with the antibody concentration of 3.9 mg/mL was added into 10 μL 1 mM SMCC PBS solution at 37 °C and kept for 2 h. After purified with cutoff membrane (10000 MW Millipore), both products were then mixed for incubation overnight and then purified with ultrafiltration (100000 MW Millipore). Finally, the antibody bound with DNA1 was collected in 100 μL PBS (55 mM phosphate , 50 mM NaCl , 5 mM EDTA , pH = 7.4). DNA2-modified antibody2 was prepared in the same procedure.

2.5. Preparation of probe 1 and probe 2

DNA3-labeled asymmetrical modification Au NPs was mixed with DNA1-labeled antibody1 in presence of Tris-HCl buffer (20 mM, PH 7.4, 10 mM Na^{+}, 10 mM Mg^{2+}) at 37 °C for 1.5 h. Centrifugation and washing process was repeated three times to achieve probe1. The procedure of obtaining probe2 was the same with probe1, replacing DNA3-labeled asymmetrical modification Au NPs with DNA4-labeled asymmetrical modification Au NPs and changing DNA1-labeled antibody1 to DNA2-labeled antibody2.

2.6. Detection of the immunoreaction between antibody and antigen

The detection of CEA was conducted as follows: CEA was diluted into various concentrations and added into the solution containing PBS, probe1 (10 pM) and probe2 (10 pM) to form immunocomplex at 37 °C for 1 h with slow shaking. Subsequently, the sample (50 μL) was dripped on the glass slide and imaged under the dark field microscope. To explore the potential application in clinic, the antigen standards of 50,

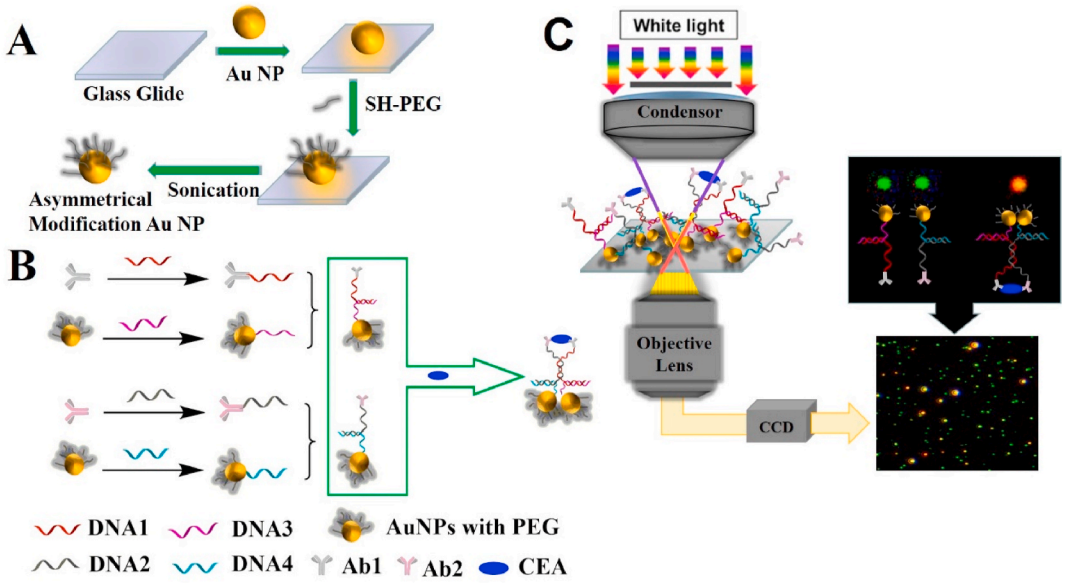

Scheme 1. (A) The preparation process of asymmetry Au NPs; (B)The process of proximity binding immunoassay-induced formation of gold nanoparticles (Au NPs) dimers; (C) Illustration of the proximity immunoassay based on the oriented assembly of Au NPs dimers and the dark-field microscope.

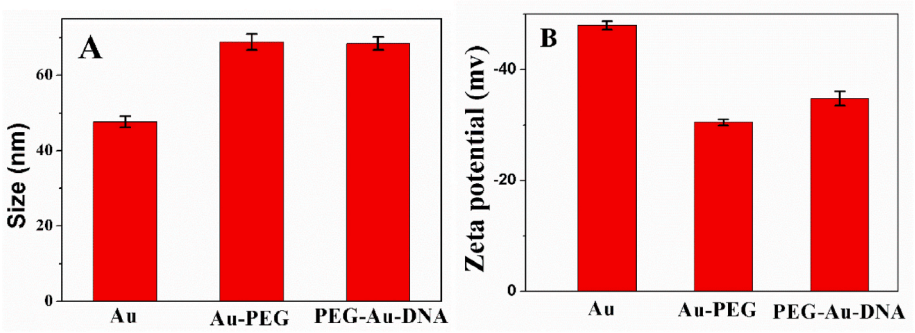

Fig. 1. Characterization of the preparation process of modified Au NPs: (A) the average mean hydrated size for AuNPs, Au-PEG, PEG-Au-DNA; (B) the zeta potential for AuNPs, Au-PEG, PEG-Au-DNA.

150 and 200 pg/mL were injected into serum sample respectively without further treatment, and the detection procedure were same as above mentioned.

3. Result and discussion

3.1. Sensing mechanism

The rationale of colorimetric assay combines the specific recognition between antibody and antigen and the perfect complementation of DNA. As illustrated in Scheme 1(A), Au NPs, immobilizing on glass glide through electrostatic attraction to reserve sites for further modification, was immersed in aqueous solution containing SH-PEG-COOH. After ultrasonic treatment, asymmetry-PEGylated Au NPs was prepared, on the surface of that a dense PEG monolayer formed except the areas contacting with the substrate. As shown in Scheme 1(B), DNA1-labled antibody was mixed with DNA3-labled asymmetry-PEGylated Au NPs to achieve probe1, due to the complementary segment between DNA1 and DNA3. The preparation procedure of probe2 is similar to that of probe1. In the presence of CEA, benefit from the affinity among anti-CEA1, anti-CEA2 and CEA, the distance of Au NPs was close enough and form dimers. This results in the generation of yellow dots under dark-field microscopy (Scheme 1C). And then, the level of CEA can be easily quantified by counting the number of scattering light spots in dark-filed microscope.

3.2. Characterization of modification

The success of modification steps is a prerequisite for the preparation of probes for CEA detection. Thus, the reactions were carefully investigated during the modification experiments of labeled Au NPs and antibody. The average size of Au NPs, Au NPs-PEG and Au NPs-PEG-DNA were first characterized using dynamic light scattering (DLS). Fig. 1A showed that the average size of Au NPs was 47.67 + 1.5 nm. After the modification of PEG, the average size of Au NPs-PEG changed to be 68.86 ± 2.1 nm, demonstrating the success modification of SH-PEG on Au NPs surface. Owing to the limited sites for DNA immobilizing on the surface of asymmetrically modified Au NPs-PEG, the change of average size from Au NPs-PEG to Au NPs-PEG-DNA (68.46 ± 1.7 nm) is unconspicuous. Based on theoretical calculations and fluorescence analysis, each Au NP monomer was calculated to carry roughly 27 ± 1 DNA strands thiol-oligonucleotides (Fig. S2 and S3). This asymmetrical modification was also studied through Zeta potential analysis. From Fig. 1B we could find a negative ζ potential (−48 mV) of Au NPs due to the negative phosphate groups on the surface of Au NPs. After the modification, the ζ potential of AuNPs-PEG changed to −30.5 mV because the modification of SH-PEG molecules which take place sodium citrate. The obtained asymmetrically modified monomer probes

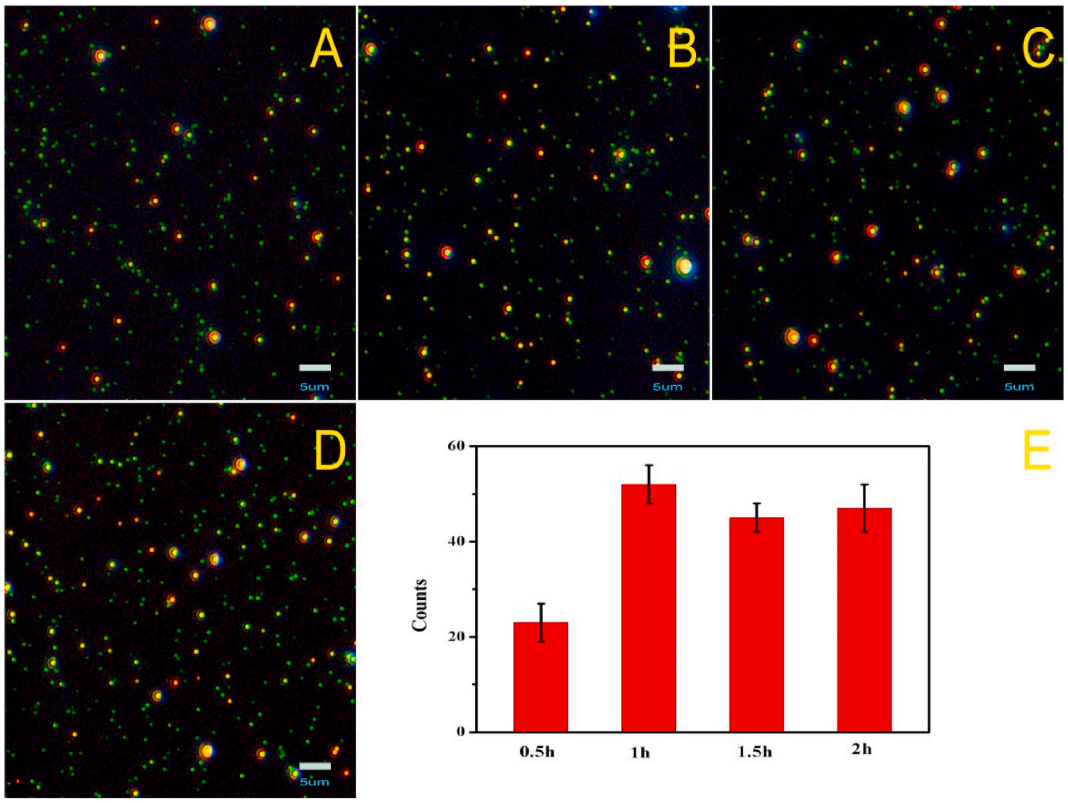

Fig. 2. The Optimization of time for immunoreaction: (A–D) the dark-field images of 0.5 h 1.0 h 1.5 h 2.0 h, in the presence of CEA (125 pg/mL), respectively; (E) Au NP dimer counts in response to reaction time.

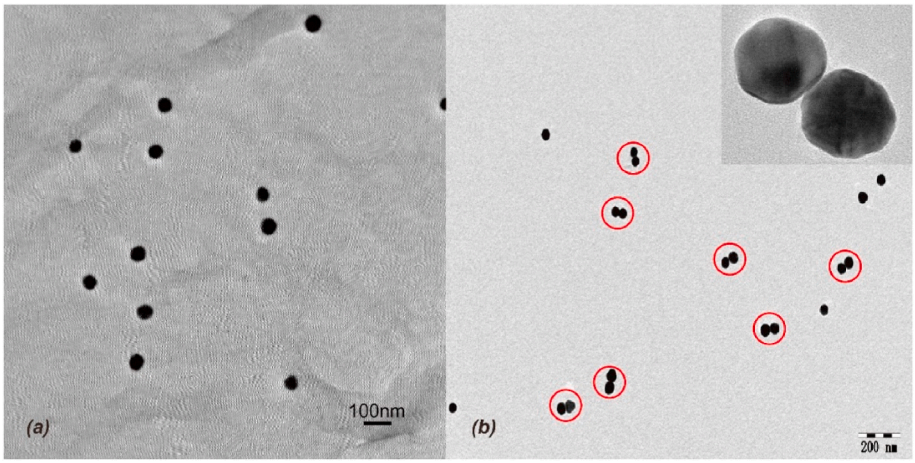

Fig. 3. TEM images of Au NPs-probes before (a) and after (b) the addition of CEA.

(AuNPs-PEG-DNA) showed slight decrease of ζ potential (−34.77 mV). The slight change was due to that only limited DNA probes with negative phosphate groups were modified on AuNPs-PEG after asymmetrical PEGylation.

3.3. Optimization of the assay conditions

Considering that it takes some time to achieve dynamic balance for immunoassay, the reaction time of CEA and anti-CEA was investigated to attain wonderful analytical performance. As shown in Fig. 2, The number of yellow spots increased when the reaction time ranged from 0.5 h to 1.0 h. However, there was no obvious difference among 1.0 h, 1.5h and 2.0 h. Thus, 1.0 h was selected as the reaction time as it was more efficient for experimental operation.

3.4. Feasibility of the proximity immunoassay

TEM images were used to verify the formation of immunocomplex (Fig. 3). As presented in Fig. 3A, probe1 and probe2 were well dispersed in the absence of CEA. Nevertheless, the existence of CEA caused the occurring of immunoreaction, diminishing the distance of inter-particles to be close enough to form Au NPs dimers (Fig. 3B and Fig. S4). In dark-filed images, the green spots correspond with Au NPs monomers and the yellow spots represent Au NPs dimers. In order to validate the correspondence of TEM and dark-field images, the plasmon resonance spectrum of green and yellow spots were recorded in Fig. 4. The result

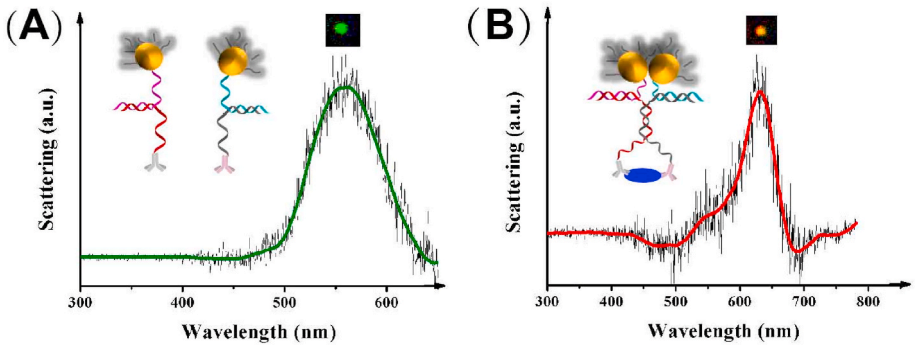

Fig. 4. Typical scattering spectrum of Au NPs monomer (A) and dimer (B).

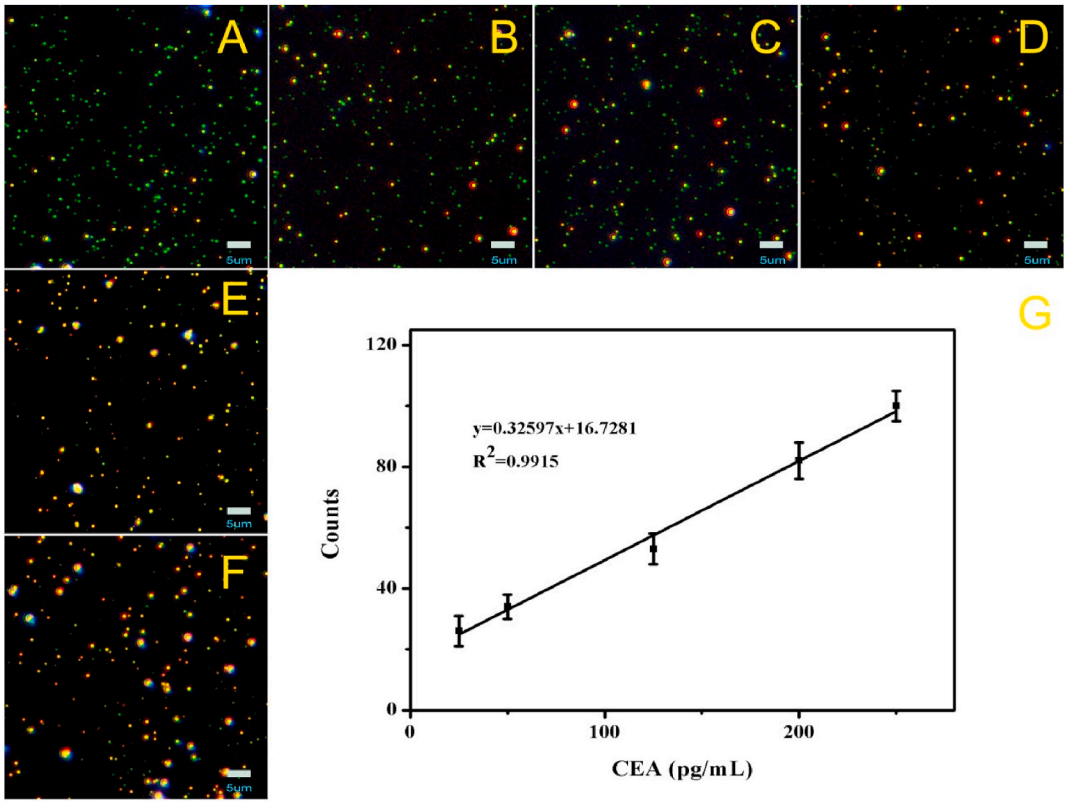

Fig. 5. (A–F) Dark-field images of Au NPs with different concentrations of CEA (0, 25, 50, 125, 200, 250 pg/mL). (G) the linear relationship between the Au NP dimer counts and the concentrations of CEA from 25 to 250 pg/mL.

revealed that the scattring peak of a monomer locate at 550 nm, being in the spectral range of green light. Meanwhile, the plasmon resonance wavelength of a dimer centering at 610 nm which locates in the spectral range of yellow light. The perfect matchup among dark-filed images, the scattering spectrum and TEM manifests the number-counting method with dark-field images is a promising tool in bioanalysis and quantification.

3.5. Quantification detection and imaging of CEA

Under optimal experimental conditions, this designed sensing system was studied with different concentrations of target CEA antigen. Ending the immunoreaction, the reaction liquid was dropped on glass slide. Since the amount of CEA is yellow-spots-relative under dark microscope, the concentration of target can thus be quantified by counting yellow spots in the dark-field image. As can be seen from Fig. 5A–F, with the increasement of CEA concentration, the number of yellow spots increased, which indicated that a growing number of Au NPs dimers formed. From Fig. 5 G, we can see that Au NPs dimer counts as a function of CEA concentration is in a linear ranged from 25 to 250 pg/mL. The limit of detection (LOD) is estimated to be 14.25 pg/mL from 3 s_b/q, (s_b is standard deviation of the blank response and q is the slope of the calibration curve). This LOD was much lower than the threshold level in serum sample from cancer patients (~10 ng/mL) [27], and was comparable with that of 0.01 ng/mL CEA by Fc-labeled biofunctionalized AuNPs based electrochemical biosensor [28]. It was also much lower than that of all-in-one dual-aptasensor with 1,1′-oxalyldiimidazole (ODI) chemiluminescence biosensor (0.58 ng/mL CEA) [29], gold nanoparticles assistant surface plasmon resonance biosensor (1.0 ng/mL CEA) [30], electrochemical sandwich CEA biosensor with concanavalin A and a DNA aptamer (3.4 ng/mL CEA) [31], and electrochemiluminescence aptasensor (0.031 ng/mL CEA) [32], or Exonuclease III-assisted fluorometric aptasensor (30 pg/mL CEA) [33]. The low LOD was attributed to the asymmetric modification of gold nanoparticles, the

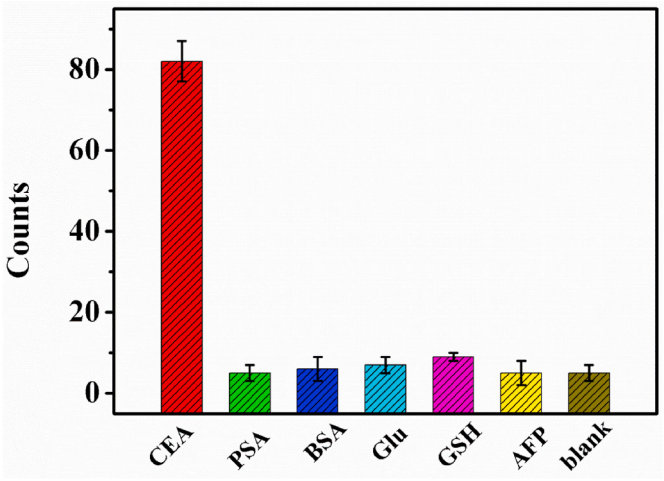

Fig. 6. Specificity assay of the proximity binding-based immunoassay. The concentrations of CEA, PSA, BSA, Glu, GSH and AFP were 200 pg/mL, respectively.

Table 1
Detection of CEA in serum samples (n = 3).

sample	spiked(pg/mL)	detected(pg/mL)	recovery(%)	RSD(%)
1	50.0	52.2	104.4	14.8
2	150.0	158.5	105.7	7.03
3	200.0	201.3	100.6	3.46

oriented assembly of dimers with the proximity binding-based immunoassay and the high resolution from dark-field microscope.

3.6. The specificity and applicability of the biosensor

Specificity is an essential element to build a bioassay method. Taking the complexity of biological samples into account, prostate specific antigen, albumin from bovine serum, glucose, glutathione and α-fetoprotein were chosen to evaluate this immunosensing assay under the same detection conditions of CEA. As presented in Fig. 6, the tested interfering species caused unconspicuous change of dimers expect the CEA. To investigate the feasibility of our project in actual samples which contain proteins, glucose salt and other potential interferences substance, CEA was spiked into human serum with standard adding method. The recovery ranges from 104.4% to 105.7% (Table 1), indicating the applicability of the design for analyzing CEA in biological samples.

4. Conclusion

We demonstrated an antigen-induced formation of Au NPs dimers strategy for ultrasensitive detection of CEA on the basis of enumerating scattering light spots of Au NPs dimers with dark-field microscope. In this proximity binding-based immunoassay, Au NPs could form dimerization and effectively enhance the plasmon coupling effect in the presence of the target, which resulting in the distinguish red-shift of scattering light in dark-filed microscope. By counting the number of scattering light spots in dark-filed microscope, a linear range of CEA from 25 to 250 pg/mL and a limit of detection of 14.25 pg/mL was obtained due to the oriented assembly of dimers with the proximity binding-based immunoassay and the high resolution with dark-field microscope. In addition, the proximity ligation needs two antibody-DNA pairs to simultaneously recognize one target protein, thus the specificity of this binding-based immunoassay has been greatly enhanced. Therefore, we believe this strategy can be applied to analyze other kinds of biomarkers individually or simultaneously using corresponding affinity probes. And it could also be easily extended to the visualization of biomarkers detection for point-of-care testing based on colorimetric substrates and has a prospective practicality in clinical biomarkers quantification.

Declaration of competing interest

The authors declare that they have no known competing financial interests or personal relationships that could have appeared to influence the work reported in this paper.

Acknowledgments

We gratefully acknowledge the support from the National Natural Science Foundation of China (Grant Nos. 21675074).

Appendix A. Supplementary data

Supplementary data to this article can be found online at https://doi.org/10.1016/j.talanta.2021.122515.

Credit statement

Hong Zhou: Conceptualization, Funding acquisition, Writing – review & editing; Qiao Yu: Conceptualization, Methodology, Investigation; Haiyan Wang: Formal analysis; Wenjing Zhu: Formal analysis; Jing Liu: Conceptualization, Writing – review & editing; Zonghua Wang: Review & editing.

References

[1] S. Fredriksson, M. Gullberg, J. Jarvius, C. Olsson, K. Pietras, S.M. Gústafsdóttir, et al., Protein detection using proximity-dependent DNA ligation assays. Nat, Biotechnol. 20 (2002) 473–477.
[2] H. Liang, S. Chen, P.P. Li, L.P. Wang, J.Y. Li, J. Li, et al., A nongenetic approach for imaging protein dimerization by aptamer recognition and proximity-induced DNA assembly, J. Am. Chem. Soc. 140 (2018) 4186–4190.
[3] J.M. Hu, T.Y. Wang, J. Kim, C. Shannon, C.J. Easley, Quantitation of femtomolar protein levels via direct readout with the electrochemical proximity assay, J. Am. Chem. Soc. 134 (2012) 7066–7072.
[4] J.M. Yang, B.T. Dou, R. Yuan, Y. Xiang, Proximity Binding, Metal Ion-Dependent, DNAzyme cyclic amplification-integrated aptasensor for label-free and sensitive electrochemical detection of thrombin, Anal. Chem. 88 (2016) 8218–8223.
[5] X.F. Wang, H.F. Gao, H.L. Qi, Q. Gao, C.X. Zhang, Proximity hybridization-regulated immunoassay for cell surface protein and protein-overexpressing cancer cells via electrochemiluminescence, Anal. Chem. 90 (2018) 3013–3018.
[6] G.-B. Hu, C.-Y. Xiong, W.-B. Liang, X.-S. Zeng, H.-L. Xu, Y. Yang, et al., Highly stable mesoporous luminescence-functionalized MOF with excellent electrochemiluminescence property for ultrasensitive immunosensor construction, ACS Appl. Mater. Interfaces 10 (2018) 15913–15919.
[7] J.Y. Xu, M. Shi, W.T. Chen, Y. Huang, L.N. Fang, L.F. Yao, et al., A gold nanoparticle-based four-color proximity immunoassay for one-step,, Multiplexed Detection of Protein Biomarkers Using Ribonuclease H Signal Amplification. Chem. Commun 54 (2018) 2719–2722.
[8] Y.S. Tian, C. Xin, S. Liu, Y. Liu, S.F. Liu, Affinity binding-induced Hg^{2+} release and quantum dot doping for general, label-free, and homogenous fluorescence protein assay, ACS Sens. 37 (2018) 1401–1408.
[9] L.M. Wei, X.Y. Wang, D. Wu, C. Li, Y.M. Yin, G.X. Li, Proximity ligation-induced assembly of DNAzymes for simple and cost-effective colourimetric detection of proteins with high sensitivity, Chem. Commun. 52 (2016), 5633–563.
[10] Q. Xiao, J. Wu, P.Y. Dang, H.X. Ju, Multiplexed chemiluminescence imaging assay of protein biomarkers using DNA microarray with proximity binding-induced hybridization chain reaction amplification, Anal. Chim. Acta 1032 (2018) 130–137.
[11] C. Zong, J. Wu, M.M. Liu, F. Yan, H.X. Ju, High-throughput imaging assay of multiple proteins via target-induced DNA assembly and cleavage, Chem. Sci. 6 (2015) 2602–2607.
[12] G.M. Wen, H.X. Ju, Enhanced photoelectrochemical proximity assay for highly selective protein detection in biological matrixes, Anal. Chem. 88 (2016) 8339–8345.
[13] B.Q. Liu, J.F. Chen, Q.H. Wei, B. Zhang, L. Zhang, D.P. Tang, Target-regulated proximity hybridization with three-way DNA junction for in situ enhanced electronic detection of marine biotoxin based on isothermal cycling signal amplification strategy. Biosens, Bioelectron 69 (2015) 241–248.
[14] Y. Qian, T. Fan, P. Wang, X. Zhang, J.J. Luo, F.Y. Zhou, et al., A novel label-free homogeneous electrochemical immunosensor based on proximity hybridization-

triggered isothermal exponential amplification induced G-quadruplex formation, Sensor. Actuator. B Chem. 248 (2017) 187–194.
[15] H.Y. Gan, J. Wu, H.X. Ju, Proximity hybridization-induced on particle DNA walker for ultrasensitive protein detection, Anal. Chim. Acta 1074 (2019) 142–149.
[16] F. L. Gao, F. Y. Zhou, S. J. Chen, Y. Yao, J. Wu, D. Y. Yin, et al., Proximity hybridization triggered rolling-circle amplification for sensitive electrochemical homogeneous immunoassay. Analyst 142(2017) 4308–4316.
[17] Y. Li, C. Jing, L. Zhang, Y.-T. Long, Resonance scattering particles as biological nanosensors in vitro and in vivo, Chem. Soc. Rev. 41 (2012) 632–642.
[18] Z.X. Chen, J.J. Li, X.Q. Chen, J.C. Cao, J.R. Zhang, Q.H. Min, et al., Single Gold@ Silver nanoprobes for real-time tracing the entire autophagy process at single-cell level, J. Am. Chem. Soc. 137 (2015) 1903–1908.
[19] H. Wu, S. Blickenstorfer, Y. Tiefenauer, R.F. Gonnelli, C. Schmidheini, L. Lüchtefeld, et al., Dark-field microwells toward high-throughput direct miRNA sensing with gold nanoparticles, ACS Sens. 4 (2019) 1950–1956.
[20] H.-Y. Jin, D.-W. Li, N. Zhang, Z. Gu, Y.-T. Long, Analyzing carbohydrate-protein interaction based on single plasmonic nanoparticle by conventional dark field microscopy, ACS Appl. Mater. Interfaces 7 (2015) 12249–12253.
[21] Y. Li, Q.Y. Liu, Z.B. Chen, Optical aptasensing of mercury(II) by using salt-induced and exonuclease I-induced gold nanoparticle aggregation under dark-field microscope observation, Microchim. Acta 186 (2019) 729.
[22] C.-Y. Poon, L. Wei, Y.L. Xu, B. Chen, L.H. Xiao, H.-W. Li, Quantification of cancer biomarkers in serum using scattering-based quantitative single particle intensity measurement with a dark-field microscope, Anal. Chem. 88 (2016) 8849–8856.
[23] X.-L. Li, Z.-L. Zhang, W. Zhao, X.-H. Xia, J.-J. Xu, H.-Y. Chen, Oriented Assembly of Invisible Probes: Towards Single mRNA Imaging in Living Cells. Chem. Sci. 7 (2016) 3256–3263.
[24] J. Ma, L. Zhan, R.S. Li, P.F. Gao, C.Z. Huang, Color-encoded assays for the simultaneous quantification of dual cancer biomarkers, Anal. Chem. 89 (2017) 8484–8489.
[25] Y.M. Han, Z.J. Ye, L.X. Chen, L.H. Xiao, Gold nanoparticles enumeration with dark-field optical microscope for the sensitive glycoprotein sandwich assay, Anal. Chim. Acta 1109 (2020) 53–60.
[26] L.H. Guo, Y. Xu, A.R. Ferhan, G.N. Chen, D.-H. Kim, Oriented gold nanoparticle aggregation for colorimetric sensors with surprisingly high analytical figures of merit, J. Am. Chem. Soc. 135 (2013) 12338–12345.
[27] R.H. Fletcher, Carcinoembryonic antigen, Ann. Intern. Med. 104 (1986) 66–73.
[28] X.F. Gu, Z. She, T.X. Ma, S. Tian, H.-B. Kraatz, Electrochemical detection of carcinoembryonic antigen. Biosens, Bioelectron 10 (2018) 610–616.
[29] H. Khang, K. Cho, S. Chong, J.H. Lee, All-in-one dual-aptasensor capable of rapidly quantifying carcinoembryonic antigen. Biosens, Bioelectron 90 (2017) 46–52.
[30] R. Li, F. Feng, Z.-Z. Chen, Y.-F. Bai, F.-F. Guo, F.-Y. Wu, et al., Sensitive detection of carcinoembryonic antigen using surface plasmon resonance biosensor with gold nanoparticles signal amplification, Talanta 140 (2015) 143–149.
[31] Q.-L. Wang, H.-F. Cui, X.J. Song, S.-F. Fan, L.-L. Chen, M.-M. Li, et al., A label-free and lectin-based sandwich aptasensor for detection of carcinoembryonic antigen, Sensor. Actuator. B Chem. 260 (2018) 48–54.
[32] Y.L. Wang, J.T. Cao, Y.H. Chen, Y.M. Liu, A label-free electrochemiluminescence aptasensor for carcinoembryonic antigen detection based on electrodeposited ZnS-CdS on MoS_2 decorated electrode. Anal, Methods 8 (2016) 5242–5247.
[33] M.J. Chen, C.B. Ma, H. Zhao, Y. Yan, Exonuclease III-assisted fluorometric aptasensor for the carcinoembryonic antigen using graphene oxide and 2-aminopurine, Microchim. Acta 186 (2019) 500.